Undamped Rabi oscillations due to polaron-emitter hybrid states in a nonlinear photonic waveguide coupled to emitters

J. Talukdar and D. Blume

Homer L. Dodge Department of Physics and Astronomy, The University of Oklahoma, 440 W. Brooks Street, Norman, Oklahoma 73019, USA and Center for Quantum Research and Technology, The University of Oklahoma, 440 W. Brooks Street, Norman, Oklahoma 73019, USA

(Received 1 March 2022; accepted 20 July 2022; published 29 July 2022)

The collective dynamics of two noninteracting two-level emitters, which are coupled to a structured wave guide that supports two-photon bound states, is investigated. Tuning the energy of the two emitters such that they are in resonance with the two-photon bound-state energy band, we identify parameter regimes where the system displays fractional populations and essentially undamped Rabi oscillations. The Rabi oscillations, which have no analog in the single-emitter dynamics, are attributed to the existence of a collective polaron-like photonic state that is induced by the emitter-photon coupling. The full dynamics is reproduced by a two-state model in which the photonic polaron interacts with the state $|e, e, \text{vac}\rangle$ (two emitters in their excited state and empty wave guide) through a Rabi coupling frequency that depends on the emitter separation. Our work demonstrates that emitter-photon coupling can lead to an all-to-all momentum space interaction between two-photon bound states and tunable non-Markovian dynamics, opening up exciting directions for emitter arrays coupled to a waveguide.

DOI: 10.1103/PhysRevA.106.013722

Multilevel emitters coupled to a radiation field in a periodic structure are essential for delivering on the promises surrounding the second quantum revolution. Ongoing research explores a variety of platforms, including nanophotonic lattices [1–5], plasmonic wave guides [6], and superconducting resonator arrays [7,8] coupled to atoms [9–11], quantum dots [12], quantum solid-state defects [13,14], or superconducting qubits [15–19]. Applications range from quantum information processing to quantum networking to quantum simulations [20–26]. Recent experimental milestones include the heralded creation of a single collective excitation in a chain of atoms coupled to a waveguide [27] and the demonstration of photon (anti) bunching for weak atom-photon coupling by taking advantage of dissipation [28]. Emitters coupled to a wave guide also constitute a promising platform with which to study fundamental questions associated with open quantum systems, with the emitters playing the role of the system and the wave guide or electromagnetic modes playing the role of the bath [29–34].

Building on the tremendous successes of cavity quantum electrodynamics (QED), waveguide QED plays a key role in a plethora of quantum technologies [35,36]. The coupling of one or more excited multilevel emitters to a continuum of electromagnetic modes leads, in most cases, to irreversible correlated radiation dynamics [37,38]. Quite generally, the strong transverse confinement in a waveguide speeds up the radiation dynamics compared to the free case [39]. Moreover, the directionality of a one-dimensional waveguide facilitates the buildup of correlations (or anticorrelations) between emitters that are separated by distances larger than the natural wave length of the wave guide leading to superradiance, subradiance, and entanglement generation [40–50]. The emergence of these characteristics can be explained in terms of constructive and destructive interferences. This work predicts long-lived oscillatory radiation dynamics for a generic waveguide QED setup that can be realized experimentally with existing state-of-the-art technology. The oscillatory radiation dynamics is distinct from the typically observed irreversible correlated radiation dynamics.

We consider a structured or nontrivial bath, namely a waveguide with nonlinearity that supports a band of two-photon bound states (or, more generally, a band of bound bath quantum pairs) [30]. Working in the quantum regime, where the system contains just two excitations, the influence of the nontrivial mode structure of the bath on the radiation dynamics is investigated within a full quantum mechanical framework. Non-Markovian dynamics is observed. Rather counterintuitively, a regime is identified where the radiation dynamics is described nearly perfectly by a two-state Rabi model. An analytical framework that elucidates the underlying physical mechanism is developed. It is shown that two emitters separated by multiple lattice sites are, in certain parameter regimes, glued together and coupled to a waveguide with all-to-all momentum space interactions. It is as if the band of two-photon bound states was feeling a localized (in real space) impurity that leads to the formation of a photonic polaron-like state with which the two-emitter unit interacts, creating hybridized symmetric and antisymmetric states that exchange population, undergoing essentially undamped Rabi oscillations.

Figure 1(a) illustrates the setup. The total Hamiltonian $\hat{H}$ consists of the system, tight-binding bath, or waveguide, and system-bath Hamiltonians $\hat{H}_s$, $\hat{H}_b$, and $\hat{H}_{sb}$ [30],

$$\hat{H}_s = \frac{\hbar\omega_e}{2}\sum_{j=1}^{N_e}\left(\hat{\sigma}_j^z + \hat{I}_j\right), \tag{1}$$

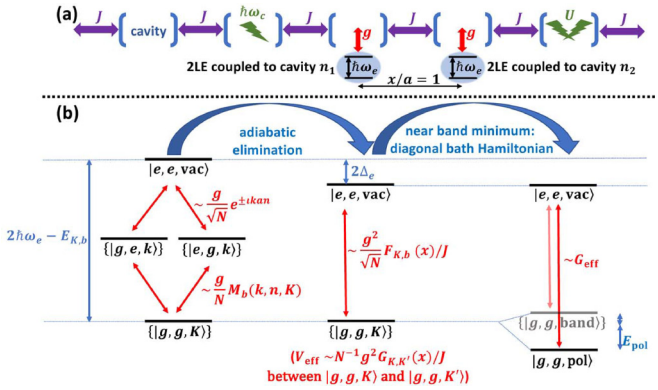

FIG. 1. (a) Schematic of the Hamiltonian $\hat{H}$. The cavity array and two-level emitters (2LE) are shown; the role of the different energy terms is illustrated. (b) Illustration of the Hilbert space structure of $\hat{H}$ (left), $\hat{H}^{\mathrm{adia}}$ (middle), and $\hat{H}^{\text{2-st.}}$ (right). The matrix element $M_b(k,n,K)$ is defined in Ref. [60]. Note that the energy difference $2\hbar\omega_e - E_{K,b}$, Stark shift $2\Delta_e$, and polaron energy E_{pol} are not shown to scale.

$$\hat{H}_b = \hbar\omega_c \sum_{n=1}^{N} \hat{a}_n^\dagger \hat{a}_n - J \sum_{n=1}^{N} (\hat{a}_n^\dagger \hat{a}_{n+1} + \hat{a}_{n+1}^\dagger \hat{a}_n) + \frac{U}{2} \sum_{n=1}^{N} \hat{a}_n^\dagger \hat{a}_n^\dagger \hat{a}_n \hat{a}_n, \tag{2}$$

and

$$\hat{H}_{sb} = g \sum_{j=1}^{N_e} (\hat{a}_{n_j} \hat{\sigma}_j^+ + \hat{a}_{n_j}^\dagger \hat{\sigma}_j^-), \tag{3}$$

where $\hbar\omega_e$, $\hbar\omega_c$, J, and U denote the energy difference of the excited and ground states of the emitter, the photon energy in the middle of the single-photon band, the hopping energy, and the engineered or intrinsic onsite energy, respectively. Since the coupling energy g is small compared to $|U|$ and J, counterrotating terms are not included in $\hat{H}_{sb}$; throughout, positive g and J and negative U are considered (positive U yield the same results). The emitter operators $\hat{\sigma}_j^z = |e\rangle_j\langle e| - |g\rangle_j\langle g|$, $\hat{I}_j = |e\rangle_j\langle e| + |g\rangle_j\langle g|$, $\hat{\sigma}_j^+ = |e\rangle_j\langle g|$, and $\hat{\sigma}_j^- = |g\rangle_j\langle e|$ act on the jth emitter located at lattice site n_j with ground and excited states $|g\rangle_j$ and $|e\rangle_j$. The bath operators $\hat{a}_{n_j}^\dagger$ and $\hat{a}_{n_j}$ create and destroy a photon at lattice site n_j ($j = 1, \ldots, N_e$ and $n_j \in 1, \ldots, N$). Throughout, we consider $N_e = 2$ emitters with separation x, $x = n_1 - n_2$, and a large number of lattice sites N. The bath Hamiltonian $\hat{H}_b$ supports, due to the Kerr-like nonlinearity U, a band of two-photon bound states, one bound state with energy $E_{K,b}$ for each two-photon center-of-mass wave vector K [51–56]. The existence of these bound states has been confirmed experimentally in photonic and cold atom optical lattice systems [57,58]. Throughout, the emitter energy is tuned such that $2\hbar\omega_e$ is equal to $E_{K^{(0)},b}$ at the uncoupled resonance wave vector $K^{(0)}$. Since we are interested in the two-excitation subspace with $K^{(0)}a$ close to zero, the detuning δ is measured from the bottom of the two-photon bound state band, $\delta = 2\hbar\omega_e - 2\hbar\omega_c + \sqrt{U^2 + 16J^2}$.

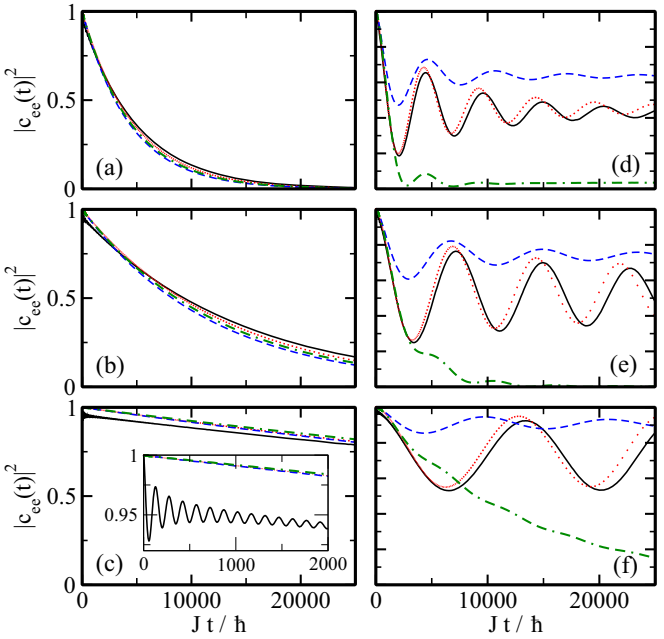

FIG. 2. $|c_{ee}(t)|^2$ as a function of $Jt/\hbar$ for the initial state $|e,e,\mathrm{vac}\rangle$, $U/J = -1$, $g/J = 1/50$, and $\delta/J = 0.0431$ (left) and $\delta/J = 0.0011$ (right). Top, middle, and bottom rows are for $x/a = 0$, 5, and 10, respectively. Black solid, red dotted, blue dashed, and green dash-dash-dotted lines are obtained using $\hat{H}$, $\hat{H}^{\mathrm{adia}}$, $\hat{H}^{\mathrm{adia}}$ with $G_{K,K'} = 0$, and $\hat{H}^{\mathrm{adia}}$ with $G_{K,K'} = \Delta_e = 0$, respectively.

To describe the time evolution of the initial state $|e,e,\mathrm{vac}\rangle$, we expand the time-dependent wave packet $|\Psi(t)\rangle$ as [30]

$$|\Psi(t)\rangle = \exp(-2\imath\omega_e t)\Big[c_{ee}|e,e,\mathrm{vac}\rangle + \sum_K c_{K,b}|g,g,K\rangle + \sum_k c_{1k}|e,g,k\rangle + \sum_k c_{2k}|g,e,k\rangle\Big], \tag{4}$$

where $c_{ee}(t)$, $c_{K,b}(t)$, $c_{1k}(t)$, and $c_{2k}(t)$ denote expansion coefficients, and $|k\rangle = \hat{a}_k^\dagger|\mathrm{vac}\rangle$ and $|K\rangle = \hat{P}_{K,b}^\dagger|\mathrm{vac}\rangle$ single-photon states with wave vector k and photon-pair states with center-of-mass wave vector K, respectively. The operators $\hat{a}_k^\dagger$ and $\hat{a}_n^\dagger$ are related via a Fourier transform. Our ansatz does not account for the two-photon scattering continuum since it plays a negligible role for the parameter combinations considered in this paper [59].

The solid lines in the left column of Fig. 2 show the population $|c_{ee}(t)|^2$ of the state $|e,e,\mathrm{vac}\rangle$ as a function of time for $U/J = -1$, $g/J = 1/50$, $\delta/J = 0.0431$, and $x/a = 0$, 5, and 10, obtained by propagating the ansatz given in Eq. (4) using $\hat{H}$. For this detuning, $|c_{ee}(t)|^2$ decreases approximately exponentially. This is the Markovian regime, discussed in Ref. [30], where propagation with the adiabatic Hamiltonian $\hat{H}^{\mathrm{adia}}$ yields quite accurate results (dotted, dashed, and dash-dash-dotted lines show results for three different variants of $\hat{H}^{\mathrm{adia}}$). The adiabatic Hamiltonian $\hat{H}^{\mathrm{adia}}$, which lives in a reduced Hilbert space that excludes the single-photon states $|e,g,k\rangle$ and $|g,e,k\rangle$, is introduced below [middle of Fig. 1(b)]. The inset of Fig. 2(c) for $x/a = 10$ shows that the short-time behavior of $|c_{ee}(t)|^2$ deviates from a pure exponential decay.

This is due to the fact that the dynamics is, for $x/a \gg 1$, seeded by the creation of two uncorrelated photons. For larger times, the fall-off is, as for smaller separations, again governed by correlated two-photon dynamics.

When the emitter energy is set such that $|\delta|$ is very small ($K^{(0)}a \approx 0$), the radiation dynamics changes drastically. The right column of Fig. 2 shows an example for $\delta/J = 0.0011$. For $x = 0$ [Fig. 2(d)], the propagation under $\hat{H}$ (solid line) yields damped oscillatory behavior. In the long-time limit, the system is characterized by fractional steady-state atomic populations. This is analogous to the single-emitter case [31,32], where the emitter frequency is in resonance with the single-photon scattering band. In the single-emitter case, the term fractional steady-state atomic population is used to indicate that the system is in a quasistationary state, which has appreciable overlap with the state $|e, \text{vac}\rangle$ and the states $|g, k\rangle$ [31]. By analogy, we use the term fractional steady-state atomic population in our two-emitter case to indicate that the system is in a quasistationary state, which has appreciable overlap with the state $|e, e, \text{vac}\rangle$ and the states $|g, g, K\rangle$. As the separation increases [Figs. 2(e) and 2(f) show results for $x/a = 5$ and 10, respectively], the dynamics for the Hamiltonian $\hat{H}$ (solid lines) are characterized by slower oscillations and weaker damping. For $x/a = 10$, the oscillations resemble nearly perfect two-state Rabi oscillations. Even though the emitters are coupled to a bath, dephasing is essentially absent for large separations. These undamped Rabi oscillations have no analog in the single-emitter system [31,32].

The oscillation frequencies in Figs. 2(d) to 2(f) correspond to the energy difference between the two energy eigenstates of $\hat{H}$ that have the largest overlap with $|e, e, \text{vac}\rangle$ [solid lines in Fig. 3(a)]; we label these states Ψ_+ and Ψ_-. For $x/a \gtrsim 5$, $\Psi_\pm$ have an energy that is smaller than $E_{K=0,b}$, i.e., both states are bound with respect to the $g = 0$ two-photon bound-state band [solid line in Fig. 3(b)]. For $x/a \lesssim 5$, the energy of Ψ_+ remains below the bottom of the two-photon band while that of Ψ_- lies in the continuum. The quantity $|\langle e, e, \text{vac}|\Psi_+\rangle|^2$ increases from about 0.66 to 0.99 as x/a increases from 0 to 20 [upper solid line in Fig. 4(a)]; $|\langle e, e, \text{vac}|\Psi_-\rangle|^2$, in contrast, is comparatively small for $x/a \lesssim 4$, increases for $x/a = 5$ to 7, and then slowly decreases as x/a increases further [lower solid line in Fig. 4(a)].

To understand the emergence of the bound states and their dependence on x, we adiabatically eliminate the states $|e, g, k\rangle$ and $|g, e, k\rangle$, i.e., we assume that the change of the expansion coefficients $c_{1k}(t)$ and $c_{2k}(t)$ in Eq. (4) with time can be neglected [30]. This introduces a Stark shift $2\Delta_e$ as well as effective momentum space interactions, proportional to $N^{-1}g^2 G_{K,K'}(x)/J$, between two-photon bound states with wave vectors K and K'. Since the two-photon bound state with wave vector K is coupled to two-photon bound states with other K', i.e., $G_{K,K'}(x)$ is nondiagonal, we refer to the effective interaction $N^{-1}g^2 G_{K,K'}(x)/J$ as an effective all-to-all momentum space interaction. The spread of $G_{K,K'}(x)$ over a wide range of center-of-mass wave vectors is discussed in detail in Ref. [61]; it plays a critical role when the absolute value of the detuning δ is small. The structures of $\hat{H}$ and the Hamiltonian $\hat{H}^{\text{adia}}$ after adiabatic elimination are sketched, respectively, in the left and middle diagrams of Fig. 1(b).

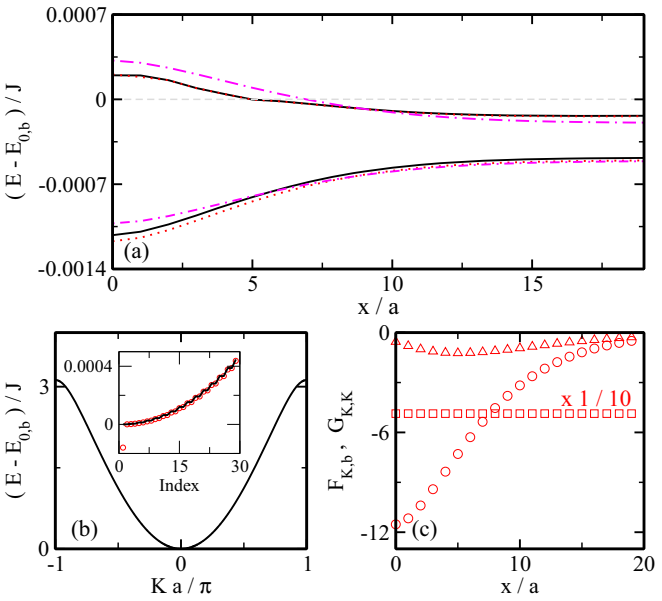

FIG. 3. Static results ($U/J = -1$, $g/J = 1/50$, and $\delta/J = 0.0011$). (a) Black solid, red dotted, and magenta dash-dotted lines show the eigenenergies corresponding to hybridized states of $\hat{H}$, $\hat{H}^{\text{adia}}$, and $\hat{H}^{\text{2-st.}}$, respectively, as a function of x/a. The gray dashed line shows $(E - E_{0,b})/J = 0$. (b) The black solid line shows $E_{K,b}$ as functions of Ka/π (main panel) and the state index (inset). The red circles show the eigenenergies supported by $\hat{H}_b^{\text{adia}}$ (index 1 corresponds to the polaron-like state). (c) The squares, circles, and triangles show the dimensionless quantities $\text{Re}[G_{K^{(0)},K^{(0)}}(x)]/10$, $\text{Re}[F_{K^{(0)},b}(x)]$, and $\text{Im}[F_{K^{(0)},b}(x)]$ as a function of x/a for $K^{(0)}a/\pi = 0.0152$.

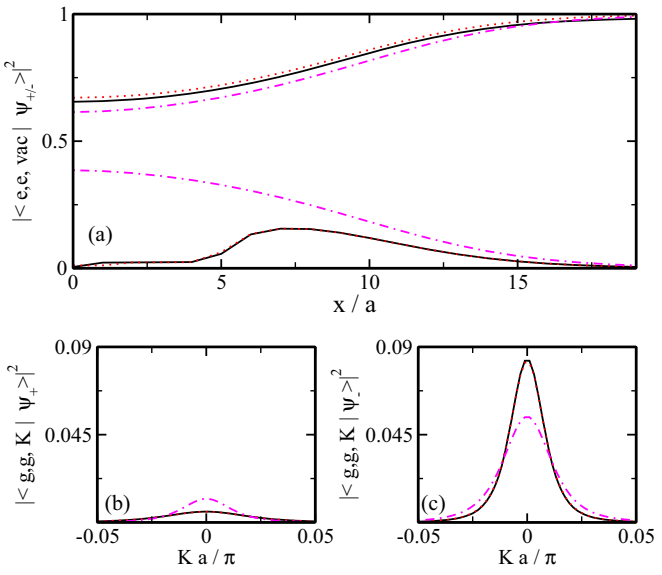

FIG. 4. State composition of hybridized polaron-emitter states ($U/J = -1$, $g/J = 1/50$, and $\delta/J = 0.0011$). (a) Projection of $|e, e, \text{vac}\rangle$ onto Ψ_+ (upper three lines) and Ψ_- (lower three lines) as a function of x/a. Black solid, red dotted, and magenta dash-dotted lines are obtained using $\hat{H}$, $\hat{H}^{\text{adia}}$, and $\hat{H}^{\text{2-st.}}$, respectively. (b), (c) Projection of Ψ_+ and Ψ_- onto $|g, g, K\rangle$ as a function of Ka/π for $x/a = 10$. The line styles are the same as in (a); black solid and red dotted lines are nearly indistinguishable on the scale shown.

For the larger δ considered in Fig. 2 (left column), the $2\Delta_e$ and $G_{K,K'}(x)$ terms have negligible effects on the radiation dynamics [the dotted, dashed, and dash-dash-dotted lines in Figs. 2(a) to 2(c) agree well]; as a consequence, the authors of Ref. [30] set them to zero in their reduced Hilbert space description. For the smaller δ (right column of Fig. 2), in contrast, both terms have a nonnegligible effect on the dynamics as evidenced by the fact that the dotted, dashed, and dash-dash-dotted lines in Figs. 2(d) to 2(f) disagree.

The adiabatic Hamiltonian $\hat{H}^{\text{adia}}$ contains the system, bath, and system-bath Hamiltonians $\hat{H}_s^{\text{adia}}$, $\hat{H}_b^{\text{adia}}$, and $\hat{H}_{sb}^{\text{adia}}$,

$$\hat{H}_s^{\text{adia}} = 2\Delta_e |e, e, \text{vac}\rangle\langle e, e, \text{vac}|, \tag{5}$$

$$\hat{H}_b^{\text{adia}} = \sum_K E_{K,b} |g, g, K\rangle\langle g, g, K| + \sum_{K,K'} \frac{g^2}{JN} G_{K,K'}(x) |g, g, K\rangle\langle g, g, K'|, \tag{6}$$

and

$$\hat{H}_{sb}^{\text{adia}} = \sum_K \frac{g^2}{J\sqrt{N}} F_{K,b}(x) |g, g, K\rangle\langle e, e, \text{vac}| + \text{H.c.} \tag{7}$$

The analytical expressions for the effective interactions $g^2 N^{-1/2} F_{K,b}(x)/J$ and $g^2 N^{-1} G_{K,K'}(x)/J$ are lengthy and not reproduced here [30,61]. The dotted lines in Figs. 2, 3(a), and 4(a) show the results obtained by propagating the initial state $|e, e, \text{vac}\rangle$ with $\hat{H}^{\text{adia}}$. The dotted lines agree quite well with the full calculation (solid lines) for all detunings and separations considered, suggesting that the reduced Hilbert space model captures the key physics. Thus, we use it to develop physical intuition.

To start with, we analyze the $K \approx K' \approx K^{(0)} \approx 0$ portion of $\hat{H}_b^{\text{adia}}$, which should govern the radiation dynamics when $|\delta/J|$ approaches zero. In this regime, the imaginary part of $G_{K,K'}(x)$ is vanishingly small. In fact, since $G_{K,K'}(x)$ is (excluding real overall factors) a sum over products $[M_b(k, n, K)]^* [M_b(k, n, K')]$, it is purely real for $K = K'$; here, $M_b(k, n, K)$ measures the overlap between $|K\rangle$ and $\hat{a}_n^\dagger |k\rangle$ [61]. When K and K' differ, $G_{K,K'}(x)$ can be loosely thought of as an autocorrelation function for the overlaps. Importantly, the real part, shown for $\delta/J = 0.0011$ by the squares in Fig. 3(c), is negative and nearly independent of x. Considering that the states $|e, g, k\rangle$ and $|g, e, k\rangle$ that are being eliminated adiabatically contain information on the emitter locations, it is remarkable that $\text{Re}[G_{K,K'}(x)]$ is nearly independent of the emitter separation x/a. The behavior of $G_{K,K'}(x)$ is discussed in detail in Ref. [61]. If we replace $E_{K,b}$ by $E_{0,b}$ (i.e., use a flat band) and $G_{K,K'}(x)$ by $G_{K^{(0)},K^{(0)}}(x)$, then the eigenenergies of the bath Hamiltonian are $E_{0,b} - (N-1)g^2 N^{-1} G_{K^{(0)},K^{(0)}}(x)/J$ (one-fold degenerate) and $E_{0,b} + g^2 N^{-1} G_{K^{(0)},K^{(0)}}(x)/J$ [$(N-1)$-fold degenerate]. The eigenstate of the one-fold degenerate bound state reads $N^{-1/2} \sum_K |K\rangle$. This bound state can be interpreted as a bosonic quasiparticle that lives in the Hilbert space of the dressed infinite cavity array, with the dressing coming from the effective photon-pair–photon-pair interactions that are introduced by the adiabatic elimination. Since the eigenstate of the bosonic quasiparticle in the cavity array Hilbert space can be written as a superposition of $|K\rangle$ states, we refer to it as a polaron-like state.

While the flat band model overestimates the binding energy of the polaron-like bound state by a fair bit, it shows that the attractive all-to-all interactions $g^2 N^{-1} G_{K,K'}(x)/J$ are responsible for the fact that the band of the bound photon pairs splits into a collective polaron-like bound state and a band that is slightly shifted upward compared to the $G_{K,K'}(x) = 0$ case. This interpretation continues to hold when a more accurate treatment is employed. The band curvature can be thought of as introducing a wave vector cutoff $(L_{\text{eff}})^{-1}$. Taylor-expanding $E_{K,b}$ up to order $(Ka)^2$, making the ansatz $|\text{pol}\rangle = \sum_K d_K |K\rangle$ with $d_K = 2N^{-1/2}(L_{\text{eff}}^{-1} a/2)^{3/2}/[(Ka)^2 + (L_{\text{eff}}^{-1} a/2)^2]$, and treating L_{eff} as a variational parameter, the energy E_{pol} of the polaron $|\text{pol}\rangle$ can be found analytically. For the parameters considered in Fig. 3(b), the analytical result is in excellent agreement with the lowest eigenenergy of $\hat{H}_b^{\text{adia}}$, which is shown in Fig. 3(b) by the circle for state index 1.

Since $G_{K^{(0)},K^{(0)}}(x)$ is, for fixed δ/J and U/J, approximately independent of x, the separation dependence displayed in Figs. 2(d) to 2(f) must enter through $F_{K^{(0)},b}(x)$. Figure 3(c) shows that $\text{Re}[F_{K^{(0)},b}(x)]$ (circles) has a strong x dependence and is much larger, in magnitude, than $\text{Im}[F_{K^{(0)},b}(x)]$ (triangles). Throughout, we work with parameter combinations where the resonant wave number $K^{(0)}$ is much smaller than a, implying that the oscillatory behavior of $F_{K^{(0)},b}(x)$, encoded in $\sin(Ka)$ and $\cos(Ka)$ terms, does not play a role [61]. This is in contrast to earlier studies where the emitter was in resonance with the single-photon band and where the oscillatory nature of the coherent and dissipative dipole-dipole interactions played a role (see, e.g., Ref. [29]). Rewriting $\hat{H}^{\text{adia}}$ in the basis in which $\hat{H}_b^{\text{adia}}$ is diagonal, we find that the state $|e, e, \text{vac}\rangle$ couples comparatively strongly to the state $|g, g, \text{pol}\rangle$ and comparatively weakly to all other bath states. The dynamics in the $|\delta/J| \to 0$ limit is thus approximately described by the two-state Hamiltonian $\hat{H}^{\text{2-st.}}$,

$$\hat{H}^{\text{2-st.}} = \hat{H}_s^{\text{adia}} + E_{\text{pol}} |g, g, \text{pol}\rangle\langle g, g, \text{pol}| + (G_{\text{eff}} |g, g, \text{pol}\rangle\langle e, e, \text{vac}| + \text{H.c.}). \tag{8}$$

Using our variational expression for $|g, g, \text{pol}\rangle$, we find

$$G_{\text{eff}} = \frac{g^3 (U^2 + 16J^2)^{1/4}}{2J^{5/2}} F_{K^{(0)},b}(x) |G_{K^{(0)},K^{(0)}}(x)|^{1/2}. \tag{9}$$

The eigenenergies of the hybridized polaron-emitter states Ψ_+ and Ψ_- supported by Eq. (8) for $U/J = -1$, $g/J = 1/50$, and $\delta/J = 0.0011$ [dash-dotted lines in Fig. 3(a)] agree reasonably well with those of $\hat{H}$ when x/a is large. State Ψ_+ is symmetric (the coefficients of $|e, e, \text{vac}\rangle$ and $|g, g, \text{pol}\rangle$ are both positive) while Ψ_- is antisymmetric (the coefficients have opposite signs).

The two-state description deteriorates with decreasing separation; the state composition of the more weakly bound state Ψ_-, which has a smaller overlap with the emitter state $|e, e, \text{vac}\rangle$ [lower three lines in Figs. 4(a) and 4(c)] than the more deeply bound state Ψ_+ [upper three lines in Figs. 4(a) and 4(b)], deviates notably from that obtained by diagonalizing $\hat{H}$. In fact, for $x/a \lesssim 5$, the first excited state of $\hat{H}$ is no longer a simple superposition of $|e, e, \text{vac}\rangle$ and $|g, g, \text{pol}\rangle$, but

instead contains multiple nearly degenerate energy eigenstates with energy close to $E_{K=0,b}$. In the dynamics, this results in dephasing, thereby explaining the damping observed in Figs. 2(d) and 2(e). We emphasize that the emergence of the three different regimes (exponential decay, fractional populations, and Rabi oscillations), illustrated in Fig. 2 for the separations of $x/a = 0$, 5, and 10, depends on the values of U/J, g/J, and δ/J. For the same U/J and δ/J, the Rabi oscillation regime can be understood by analyzing the interplay between $E_{\rm pol}$ (which contains a term that scales as $-g^4/J^4$), $G_{\rm eff}$ (which is proportional to g^3/J^3), and Δ_e (which is proportional to g^2/J^2) within the two-state Hamiltonian $\hat{H}^{\text{2-st.}}$ [61].

In summary, our analysis shows that the essentially undamped Rabi oscillations are associated with population exchange between two hybridized polaron-emitter states. These states are distinct from previously predicted hybridized states [29,62–66]. For the parameters considered in this paper, the more weakly bound hybridized state merges into the continuum for $x/a \lesssim 5$, making the emergence of long-lived Rabi oscillations an intriguing emitter separation-dependent long-range phenomenon. When the emitters are close together, the radiation dynamics, starting with $|e, e, \text{vac}\rangle$ at $t = 0$, leads to quasistationary fractional populations. When the emitters are spaced further apart, regular revivals are observed. We emphasize the crucial role of the Stark shift $2\Delta_e$ and the attractive all-to-all momentum space interactions. Neglecting these terms yields the dash-dotted lines in Figs. 2(d) to 2(f). Setting $2\Delta_e$ to the correct value but using $G_{K,K'}(x) = 0$ yields the dashed lines.

Our work illustrates that the structure of the bath Hamiltonian with Kerr-like nonlinearity can be modified nontrivially (introducing attractive all-to-all momentum space interactions) through the coupling to two two-level emitters, resulting in qualitatively new radiation dynamics. Continuing to work in the two-excitation manifold, extension to arrays of regularly spaced emitters where neighboring emitters have a fixed separation (simple emitter lattice) or alternating separations (emitter superlattice) offers the prospect of establishing nontrivial bath-induced correlations between separated emitter pairs. Taking an alternative viewpoint, this work points toward utilizing emitters to create bath Hamiltonian with unique characteristics. Our analysis assumes that losses from the wave guide can be neglected. Over the timescales considered, this should be justified for several state-of-the-art experiments.

Support by the National Science Foundation through Grant No. PHY-1806259 is gratefully acknowledged. This work used the OU Supercomputing Center for Education and Research (OSCER) at the University of Oklahoma (OU). A discussion with Kieran Mullen on impurities in solid-state systems is gratefully acknowledged.

[1] D. Roy, C. M. Wilson, and O. Firstenberg, Colloquium: Strongly interacting photons in one-dimensional continuum, Rev. Mod. Phys. **89**, 021001 (2017).

[2] E. Shahmoon, P. Grišins, H. P. Stimming, I. Mazets, and G. Kurizki, Highly nonlocal optical nonlinearities in atoms trapped near a waveguide, Optica **3**, 725 (2016).

[3] F. Lombardo, F. Ciccarello, and G. M. Palma, Photon localization versus population trapping in a coupled-cavity array, Phys. Rev. A **89**, 053826 (2014).

[4] P. Longo, P. Schmitteckert, and K. Busch, Few-Photon Transport in Low-Dimensional Systems: Interaction-Induced Radiation Trapping, Phys. Rev. Lett. **104**, 023602 (2010).

[5] H. Zheng, D. J. Gauthier, and H. U. Baranger, Waveguide QED: Many-body bound-state effects in coherent and Fock-state scattering from a two-level system, Phys. Rev. A **82**, 063816 (2010).

[6] D. Chang, A. S. Sørensen, E. Demler, and M. D. Lukin, A single-photon transistor using nanoscale surface plasmons, Nat. Phys. **3**, 807 (2007).

[7] L. Zhou, Z. R. Gong, Y.-X. Liu, C. P. Sun, and F. Nori, Controllable Scattering of a Single Photon inside a One-Dimensional Resonator Waveguide, Phys. Rev. Lett. **101**, 100501 (2008).

[8] J.-T. Shen and S. Fan, Coherent Single Photon Transport in a One-Dimensional Waveguide Coupled with Superconducting Quantum Bits, Phys. Rev. Lett. **95**, 213001 (2005).

[9] D. Reitz, C. Sayrin, R. Mitsch, P. Schneeweiss, and A. Rauschenbeutel, Coherence Properties of Nanofiber-Trapped Cesium Atoms, Phys. Rev. Lett. **110**, 243603 (2013).

[10] R. Yalla, M. Sadgrove, K. P. Nayak, and K. Hakuta, Cavity Quantum Electrodynamics on a Nanofiber using a Composite Photonic Crystal Cavity, Phys. Rev. Lett. **113**, 143601 (2014).

[11] J. D. Hood, A. Goban, A. Asenjo-Garcia, M. Lu, S.-P. Yu, D. E. Chang, and H. J. Kimble, Atom-atom interactions around the band edge of a photonic crystal waveguide, Proc. Natl. Acad. Sci. USA **113**, 10507 (2016).

[12] P. Lodahl, S. Mahmoodian, and S. Stobbe, Interfacing single photons and single quantum dots with photonic nanostructures, Rev. Mod. Phys. **87**, 347 (2015).

[13] P. E. Barclay, K.-M. Fu, C. Santori, and R. G. Beausoleil, Hybrid photonic crystal cavity and waveguide for coupling to diamond NV-centers, Opt. Express **17**, 9588 (2009).

[14] B. J. M. Hausmann, B. J. Shields, Q. Quan, Y. Chu, N. P. de Leon, R. Evans, M. J. Burek, A. S. Zibrov, M. Markham, D. J. Twitchen, H. Park, M. D. Lukin, and M. Loncr, Coupling of NV Centers to Photonic Crystal Nanobeams in Diamond, Nano Lett. **13**, 5791 (2013).

[15] O. Astafiev Jr., A. M. Zagoskin, A. A. Abdumalikov, Y. A. Pashkin, T. Yamamoto, K. Inomata, Y. Nakamura, and J. S. Tsai, Resonance fluorescence of a single artificial atom, Science **327**, 840 (2010).

[16] I.-C. Hoi, C. M. Wilson, G. Johansson, T. Palomaki, B. Peropadre, and P. Delsing, Demonstration of a Single- Photon Router in the Microwave Regime, Phys. Rev. Lett. **107**, 073601 (2011).

[17] J. A. Mlynek, A. A. Abdumalikov, C. Eichler, and A. Wallraff, Observation of Dicke superradiance for two artificial atoms in a cavity with high decay rate, Nat. Commun. **5**, 5186 (2014).

[18] M. Mirhosseini, E. Kim, X. Zhang, A. Sipahigil, P. B. Dieterle, A. J. Keller, A. Asenjo-Garcia, D. E. Chang, and O. Painter, Cavity quantum electrodynamics with atom-like mirrors, Nature (London) **569**, 692 (2019).

[19] N. M. Sundaresan, R. Lundgren, G. Zhu, A. V. Gorshkov, and A. A. Houck, Interacting Qubit-Photon Bound States with Superconducting Circuits, Phys. Rev. X **9**, 011021 (2019).

[20] J. Douglas, H. Habibian, C.-L. Hung, A. V. Gorshkov, H. J. Kimble, and D. E. Chang, Quantum many-body models with cold atoms coupled to photonic crystals, Nat. Photon. **9**, 326 (2015).

[21] Y. Chougale, J. Talukdar, T. Ramos, and R. Nath, Dynamics of Rydberg excitations and quantum correlations in an atomic array coupled to a photonic crystal waveguide, Phys. Rev. A **102**, 022816 (2020).

[22] A. Gonzalez-Tudela, D. Martin-Cano, E. Moreno, L. Martin-Moreno, C. Tejedor, and F. J. Garcia-Vidal, Entanglement of Two Qubits Mediated by One-Dimensional Plasmonic Waveguides, Phys. Rev. Lett. **106**, 020501 (2011).

[23] K. Stannigel, P. Rabl, and P. Zoller, Driven-dissipative preparation of entangled states in cascaded quantum-optical networks, New J. Phys. **14**, 063014 (2012).

[24] H. Zheng and H. U. Baranger, Persistent Quantum Beats and Long-Distance Entanglement from Waveguide- Mediated Interactions, Phys. Rev. Lett. **110**, 113601 (2013).

[25] E. Shahmoon and G. Kurizki, Nonradiative interaction and entanglement between distant atoms, Phys. Rev. A **87**, 033831 (2013).

[26] P. Facchi, M. S. Kim, S. Pascazio, F. V. Pepe, D. Pomarico, and T. Tufarelli, Bound states and entanglement generation in waveguide quantum electrodynamics, Phys. Rev. A **94**, 043839 (2016).

[27] N. V. Corzo, J. Raskop, A. Chandra, A. S. Sheremet, B. Gouraud, and J. Laurat, Waveguide-coupled single collective excitation of atomic arrays, Nature (London) **566**, 359 (2019).

[28] A. S. Prasad, J. Hinney, S. Mahmoodian, K. Hammerer, S. Rind, P. Schneeweiss, A. S. Sørensen, J. Volz, and A. Rauschenbeutel, Correlating photons using the collective nonlinear response of atoms weakly coupled to an optical mode, Nat. Photon. **14**, 719 (2020).

[29] G. Calajó, F. Ciccarello, D. Chang, and P. Rabl, Atom-field dressed states in slow-light waveguide QED, Phys. Rev. A **93**, 033833 (2016).

[30] Z. Wang, T. Jaako, P. Kirton, and P. Rabl, Supercorrelated Radiance in Nonlinear Photonic Waveguides, Phys. Rev. Lett. **124**, 213601 (2020).

[31] S. John and T. Quang, Spontaneous emission near the edge of a photonic band gap, Phys. Rev. A **50**, 1764 (1994).

[32] A. G. Kofman, G. Kurizki, and B. Sherman, Spontaneous and Induced Atomic Decay in Photonic Band Structures, J. Mod. Opt. **41**, 353 (1994).

[33] A. González-Tudela and J. I. Cirac, Quantum Emitters in Two-Dimensional Structured Reservoirs in the Non-perturbative Regime, Phys. Rev. Lett. **119**, 143602 (2017).

[34] O. A. Iversen and T. Pohl, Strongly Correlated States of Light and Repulsive Photons in Chiral Chains of Three-Level Quantum Emitters, Phys. Rev. Lett. **126**, 083605 (2021).

[35] I. Carusotto, A. A. Houck, A. J. Kollár, P. Roushan, D. I. Schuster, and J. Simon, Photonic materials in circuit quantum electrodynamics, Nat. Phys. **16**, 268 (2020).

[36] R. Ma, B. Saxberg, C. Owens, N. Leung, Y. Lu, J. Simon, and D. I. Schuster, A dissipatively stabilized Mott insulator of photons, Nature (London) **566**, 51 (2019).

[37] R. H. Dicke, Coherence in spontaneous radiation processes, Phys. Rev. **93**, 99 (1954).

[38] F. W. Cummings, Spontaneous emission from a single two-level atom in the presence of N initially unexcited identical atoms, Phys. Rev. A **33**, 1683 (1986).

[39] A. S. Sheremet, M. I. Petrov, I. V. Iorsh, A. V. Poshakinskiy, and A. N. Poddubny, Waveguide quantum electrodynamics: collective radiance and photon-photon correlations, arXiv:2103.06824.

[40] K. Sinha, P. Meystre, E. A. Goldschmidt, F. K. Fatemi, S. L. Rolston, and P. Solano, Non-Markovian Collective Emission from Macroscopically Separated Emitters, Phys. Rev. Lett. **124**, 043603 (2020).

[41] H. Pichler, T. Ramos, A. J. Daley, and P. Zoller, Quantum optics of chiral spin networks, Phys. Rev. A **91**, 042116 (2015).

[42] H. R. Haakh, S. Faez, and V. Sandoghdar, Polaritonic normal-mode splitting and light localization in a one-dimensional nanoguide, Phys. Rev. A **94**, 053840 (2016).

[43] A. V. Poshakinskiy, J. Zhong, and A. N. Poddubny, Quantum Chaos Driven by Long-Range Waveguide-Mediated Interactions, Phys. Rev. Lett. **126**, 203602 (2021).

[44] A. N. Poddubny, Quasiflat band enabling subradiant two-photon bound states, Phys. Rev. A **101**, 043845 (2020).

[45] A. Goban, C.-L. Hung, J. D. Hood, S.-P. Yu, J. A. Muniz, O. Painter, and H. J. Kimble, Superradiance for Atoms Trapped along a Photonic Crystal Waveguide, Phys. Rev. Lett. **115**, 063601 (2015).

[46] A. Albrecht, L. Henriet, A. Asenjo-Garcia, P. B. Dieterle, O. Painter, and D. E. Chang, Subradiant states of quantum bits coupled to a one-dimensional waveguide, New J. Phys. **21**, 025003 (2019).

[47] M. Bello, G. Platero, J. I. Cirac, and A. González-Tudela, Unconventional quantum optics in topological waveguide QED, Sci. Adv. **5**, eaaw0297 (2019).

[48] J. Zhong, N. A. Olekhno, Y. Ke, A. V. Poshakinskiy, C. Lee, Y. S. Kivshar, and A. N. Poddubny, Photon-Mediated Localization in Two-Level Qubit Arrays, Phys. Rev. Lett. **124**, 093604 (2020).

[49] Y.-X. Zhang and K. Mølmer, Theory of Subradiant States of a One-Dimensional Two-Level Atom Chain, Phys. Rev. Lett. **122**, 203605 (2019).

[50] Y.-X. Zhang, C. Yu, and K. Mølmer, Subradiant bound dimer excited states of emitter chains coupled to a one-dimensional waveguide, Phys. Rev. Research **2**, 013173 (2020).

[51] R. Y. Chiao, I. H. Deutsch, and J. C. Garrison, Two-Photon Bound State in Self-Focusing Media, Phys. Rev. Lett. **67**, 1399 (1991).

[52] I. H. Deutsch, R. Y. Chiao, and J. C. Garrison, Diphotons in a Nonlinear Fabry-Pérot Resonator: Bound States of Interacting Photons in an Optical "Quantum Wire", Phys. Rev. Lett. **69**, 3627 (1992).

[53] R. Piil and K. Mølmer, Tunneling couplings in discrete lattices, single-particle band structure, and eigenstates of interacting atom pairs, Phys. Rev. A **76**, 023607 (2007).

[54] N. Nygaard, R. Piil, and K. Mølmer, Two-channel Feshbach physics in a structured continuum, Phys. Rev. A **78**, 023617 (2008).

[55] M. Valiente and D. Petrosyan, Two-particle states in the Hubbard model, J. Phys. B: At. Mol. Opt. Phys. **41**, 161002 (2008).

[56] D. Petrosyan, B. Schmidt, J. R. Anglin, and M. Fleischhauer, Quantum liquid of repulsively bound pairs of particles in a lattice, Phys. Rev. A **76**, 033606 (2007).

[57] O. Firstenberg, T. Peyronel, Q.-Y. Liang, A. V. Gorshkov, M. D. Lukin, V. Vuletić, Attractive photons in a quantum nonlinear medium, Nature (London) **502**, 71 (2013).

[58] K. Winkler, G. Thalhammer, F. Lang, R. Grimm, J. H. Denschlag, A. J. Daley, A. Kantian, H. P. Büchler, and P. Zoller, Repulsively bound atom pairs in an optical lattice, Nature (London) **441**, 853 (2006).

[59] We note that the authors of Ref. [30] presented a benchmark plot (Fig. 4 of the Supplemental Material) that was obtained by accounting for the scattering continuum. In addition, the authors of Ref. [30] noted that the contributions from the scattering states were confirmed to be small for the parameter combinations considered. Our calculations support these statements.

[60] The matrix element $M_b(k, n, K)$ used in our work is by a factor of N larger than that defined in Eq. (25) of the Supplemental Material of Ref. [30]. The definition employed by us (see also Ref. [61]) makes the value of $M_b(k, n, K)$ for a given ka and Ka independent of the number of lattice sites N.

[61] J. Talukdar and D. Blume, Two emitters coupled to a bath with Kerr-like nonlinearity: Exponential decay, fractional populations, and Rabi oscillations, Phys. Rev. A **105**, 063501 (2022).

[62] S. Mahmoodian, G. Calajó, D. E. Chang, K. Hammerer, and A. S. Sørensen, Dynamics of Many-Body Photon Bound States in Chiral Waveguide QED, Phys. Rev. X **10**, 031011 (2020).

[63] S.-S. Wen, Y.-G. Huang, X.-Y. Wang, J. Liu, Y. Li, X.-E. Quan, H. Yang, J.-Z. Peng, K. Deng, and H.-P. Zhao, Bound state and non-Markovian dynamics of a quantum emitter around a surface plasmonic nanostructure, Opt. Express **28**, 6469 (2020).

[64] D. Lonigro, P. Facchi, A. D. Greentree, S. Pascazio, F. V. Pepe, and D. Pomarico, Photon-emitter dressed states in a closed waveguide, Phys. Rev. A **104**, 053702 (2021).

[65] M. Stewart, J. Kwon, A. Lanuza, and D. Schneble, Dynamics of matter-wave quantum emitters in a structured vacuum, Phys. Rev. Research **2**, 043307 (2020).

[66] A. Javadi, I. Söllner, M. Arcari, S. L. Hansen, L. Midolo, S. Mahmoodian, G. Kiršanskė, T. Pregnolato, E. H. Lee, J. D. Song, S. Stobbe, and P. Lodahl, Single-photon non-linear optics with a quantum dot in a waveguide, Nat. Commun. **6**, 8655 (2015).